# Novel UV Initiator for Functionalization of Multiwalled Carbon Nanotubes by Atom Transfer Radical Polymerization Applied on Two Different Grades of Nanotubes

**ANDERS E. DAUGAARD,[1] KATJA JANKOVA,[1] JESPER BØGELUND,[2] JENS KROMANN NIELSEN,[2] SØREN HVILSTED[1]**

[1]Danish Polymer Centre, Department of Chemical and Biochemical Engineering, Technical University of Denmark,
Building 227, Sølvtofts Plads, DK-2800 Kgs. Lyngby, Denmark

[2]Danish Technological Institute, Taastrup, Gregersensvej 3, DK-2630 Taastrup, Denmark

Received 8 July 2010; accepted 23 July 2010
DOI: 10.1002/pola.24257

**ABSTRACT:** A novel nonoxidative method for preparation of functionalized multiwalled carbon nanotubes (MWCNT) has been developed based on a UV sensitive initiator for atom transfer radical polymerization (ATRP). The method has been investigated with respect to ligands and polymerization time for the preparation of polystyrene functionalized MWCNT. It was found that pentamethyldiethylenetriamine (PMDETA) gave superior results with higher loading in shorter polymerization time. A comparative study of the method applied on two different grades of nonoxidized MWCNT has been performed, illustrating large differences in reactivity and polymer loading, underlining the importance of the choice of MWCNT starting material. In addition to styrene, also poly(ethylene glycol) methacrylate (PEGMA) was shown to polymerize from the surface of the MWCNT. Finally, initial results from composites of polystyrene or polyphenylenesulfide are presented. © 2010 Wiley Periodicals, Inc. J Polym Sci Part A: Polym Chem 48: 4594–4601, 2010

**KEYWORDS:** atom transfer radical polymerization; composites; multiwalled carbon nanotubes; polystyrene; surface initiation; ultra violet light

---

**INTRODUCTION** The use of carbon nanotubes (CNT) to reinforce materials has received much attention in recent years. The possibility of reinforcing polymers with these extremely strong additives and obtaining composites of superior properties is very appealing. Many publications within the field illustrate that the potential could be realized, however, so far the improvements seen in mechanical properties are still inferior to what is expected to be the potential of CNT composites.[1]

In preparation of nanocomposites, it is of crucial importance to have a proper dispersion of the multiwalled carbon nanotubes (MWCNT) in the polymer matrix to gain the full effect of the additive.[2] It is one of the general beliefs that to obtain a good incorporation of CNTs in a composite, it is necessary to surface modify the CNT to obtain a good dispersion and possibly load transfer from the matrix to the CNT. For composites prepared through step growth polymerization, the incorporation of an additive can be obtained by low-molecular weight prepolymerization functionalization of the CNT material[3,4] or by grafting of the CNT material during the polymerization,[5] enabling covalent incorporation into the matrix during polymerization. If a direct covalent bond from matrix to CNT is not possible, covalent anchoring of a similar or compatible polymer would be expected to give the best results. Functionalization of CNTs can be done through a number of methods.[6,7] Often the reported methods are combined with acid treatments to purify the tubes prior to reaction. These methods are known to cause degradation and generate defects in the CNT and to introduce chemical groups such as acids, esters, anhydrides etc. in proximity to the defects. Grafting with polymers from CNTs have primarily been performed through "graft from" strategies by controlled polymerization.[8] These are mainly based on atom transfer radical polymerizations[9–19] (ATRP), but also nitroxide-mediated polymerizations[20] (NMP), reversible addition fragmentation chain-tranfer (RAFT) polymerizations,[21,22] and ring-opening polymerization[23,24] have been applied. In addition to this, there are some examples of "graft to" strategies by ATRP, NMP, and RAFT.[11,12,25–27] However, in many cases, both the polymerization and polymer grafting methods are performed on CNTs that have been through a purification step involving oxidative conditions resulting in a reduction in the aspect ratio of the CNT. A few exceptions to this procedure exist, and in these cases, either radical reactions or Diels–Alder reactions have been applied for grafting to pristine tubes.[11,28]

Herein, we present a nonoxidative method for functionalization of MWCNT, that preserves the tubes and prevent

Correspondence to: S. Hvilsted (E-mail: sh@kt.dtu.dk)
Journal of Polymer Science: Part A: Polymer Chemistry, Vol. 48, 4594–4601 (2010) © 2010 Wiley Periodicals, Inc.

reductions in the aspect ratio. A novel radical method has been developed for CNT and used to couple an initiator for ATRP onto the surface of MWCNT. The method has been applied in ATRP on two different grades of MWCNT having very different aspect ratios. Finally, initial results from preparation of composites of polystyrene (PS) or polyphenylenesulfide (PPS) and the PS-grafted MWCNT are presented.

## EXPERIMENTAL

### Materials and General Methods

All chemicals were acquired from Sigma-Aldrich and used as received unless otherwise specified. PPS was purchased from Witcom (Netherlands). Two batches of MWCNT prepared by chemical vapor deposition have been used in these investigations, a high-quality sample from Sigma-Aldrich (110–170 nm × 5-9 $\mu$m) and an industrial grade MWCNT from Nanocyl (Belgium) (9.5 nm × 1.5 $\mu$m).

Scanning electron microscopy (SEM) was performed on a Zeiss Ultra 55 SEM equipped with a field emission electron source. High vacuum conditions were applied, and a secondary electron detector was used for image acquisition. The samples were prepared on a carbon tape surface and coated with a conductive layer of Au with approximately 20 nm thickness. Thermogravimetric analysis (TGA) was performed on a TGA Q500 from TA instruments under $N_2$ with a heating rate of 10 K/min. For TGA-GC-MS a Mettler Toledo TGA/SDTA 851e was applied for the TGA from 25 to 800 °C at 10 K/min under nitrogen flow, while the off-gas was passed through adsorption columns for subsequent analysis by thermal desorption GC-MS. The collection of the degradation products was divided over temperature intervals corresponding to the weight loss steps detected in the TGA analysis. Tenax TA 300 mg filters were analyzed by thermal desorption (Perkin–Elmer ATD 400) in combination with gas chromatography on a Varian CP Sil 8 CB capillary (30 m × 0.25 mm × 0.5 $\mu$m) with a mass spectrometry detector (Perkin–Elmer Turbomass GC-MS). The amount of styrene was quantified against external standards prepared on Tenax filters. Differential scanning calorimetry (DSC) was performed on a DSC Q1000 from TA Instruments. DSC analyses were performed at a heating and cooling rate of 10 K/min. Glass transition temperatures ($T_g$s) were measured at the inflection point. Size exclusion chromatography (SEC) was performed in THF on a Viscotec model 200 operating in THF on two Polymer Laboratories PLgel 5 $\mu$m MIXED-D columns at a flow rate of 1 mL/min. A refractive index/viscometry detector and a PS calibration were used to determine $M_n$ and PDI. Raman spectra were recorded on a Thermo DXR dispersive Raman microscope with a 780 nm laser. Small amplitude oscillatory shear measurements were made on an AR2000 rheometer from TA Instruments using parallel plate geometry with a diameter of 25 mm and a plate separation of 1 mm. The measurements were performed at 200 °C and frequency sweep between 0.01 rad/s and 100 rad/s were made at a low strain of 2%.

### MWCNT-Br General Procedure

MWCNT (0.500 g) was dispersed in a toluene (20 mL) solution of benzophenonyl 2-bromoisobutanoate[29] (10 mg/mL, 0.03 M). The dispersion was stirred under UV (365 nm, 0.8 mW/cm$^2$) for up to 60 min. The dispersion was then filtered on a 0.4 $\mu$m PTFE filter, the isolated MWCNT-Br was rinsed with a generous amount of toluene and $CH_2Cl_2$ and dried *in vacuo*. The product was used without further purification.

### MWCNT-PS General Procedure

MWCNT-Br (0.156 g) was dispersed in styrene (5 mL) with CuBr (0.023 g, 0.16 mmol) and 4,4′-dinonylbipyridine (dNbiPy, 0.177 g, 0.40 mmol). The reaction mixture was frozen in liquid nitrogen, and oxygen was removed through three freeze-thaw cycles. The polymerizations were conducted under nitrogen at 110 °C for varied reaction times. After polymerization the grafted MWCNTs were reclaimed by filtration and rinsed with copious amounts of toluene and $CH_2Cl_2$. The isolated product was characterized by TGA.

### Hydrolysis of MWCNT-PS

MWCNT-PS (38 mg, 47 wt % loaded) was hydrolyzed in a mixture of KOH (1 g) and THF/ethanol (50 mL/5 mL) at 60 °C for 16 h. The mixture was concentrated, and the hydrolyzed polymer was dissolved in THF and analyzed by SEC.

### MWCNT-PPEGMA

MWCNT-Br (0.156 g) and poly(ethylene glycol) methacrylate (PEGMA, $M_n = 360$ g/mol, 2.0 mL, 5.3 mmol) was dispersed in methanol (2.5 mL) with CuCl (0.008 g, 0.08 mmol) and dNbiPy (0.032 g, 0.08 mmol). The reaction mixture was frozen in liquid nitrogen, and oxygen was removed through five freeze-thaw cycles. The polymerization was conducted under nitrogen at 30 °C for 2 h. After polymerization, the grafted MWCNTs were recovered by filtration and rinsed with copious amounts of $H_2O$ and methanol. The isolated product was characterized by TGA.

### Nanocomposite Preparation

Before processing, the PPS was dried at 160 °C for 4 h. Masterbatches were prepared by mixing in a corotating twin screw extruder Bernstorff ø 25 mm, L/D = 48 with the temperatures of heating zones 310, 310, 315, 315, 320, 320, 320, 330, 330, and 335 °C and at 100 rpm. Compositions of the masterbatches were 97.5/2.5 wt % (PPS/MWCNT).

## RESULTS AND DISCUSSION

Two batches of MWCNTs were investigated with SEM and Raman spectroscopy and as can be seen from Figure 1, the two materials are very different. In the scanning electron micrograph of the MWCNT from Sigma-Aldrich (A), it is clear that these tubes have the lowest aspect ratio with an average diameter of 110–170 nm and an average length of 5–9 $\mu$m. Compared with these, the MWCNT from Nanocyl (B) are much smaller with an average diameter and length of 9.5 nm and 1.5 $\mu$m, respectively. Similarly, the Raman spectra of the two batches also illustrate large differences. Both show the characteristic peaks of MWCNT with a G-band indicating in-plane stretching at around 1590 cm$^{-1}$ and a D-band corresponding to the sp$^3$ hybridized carbon or defects

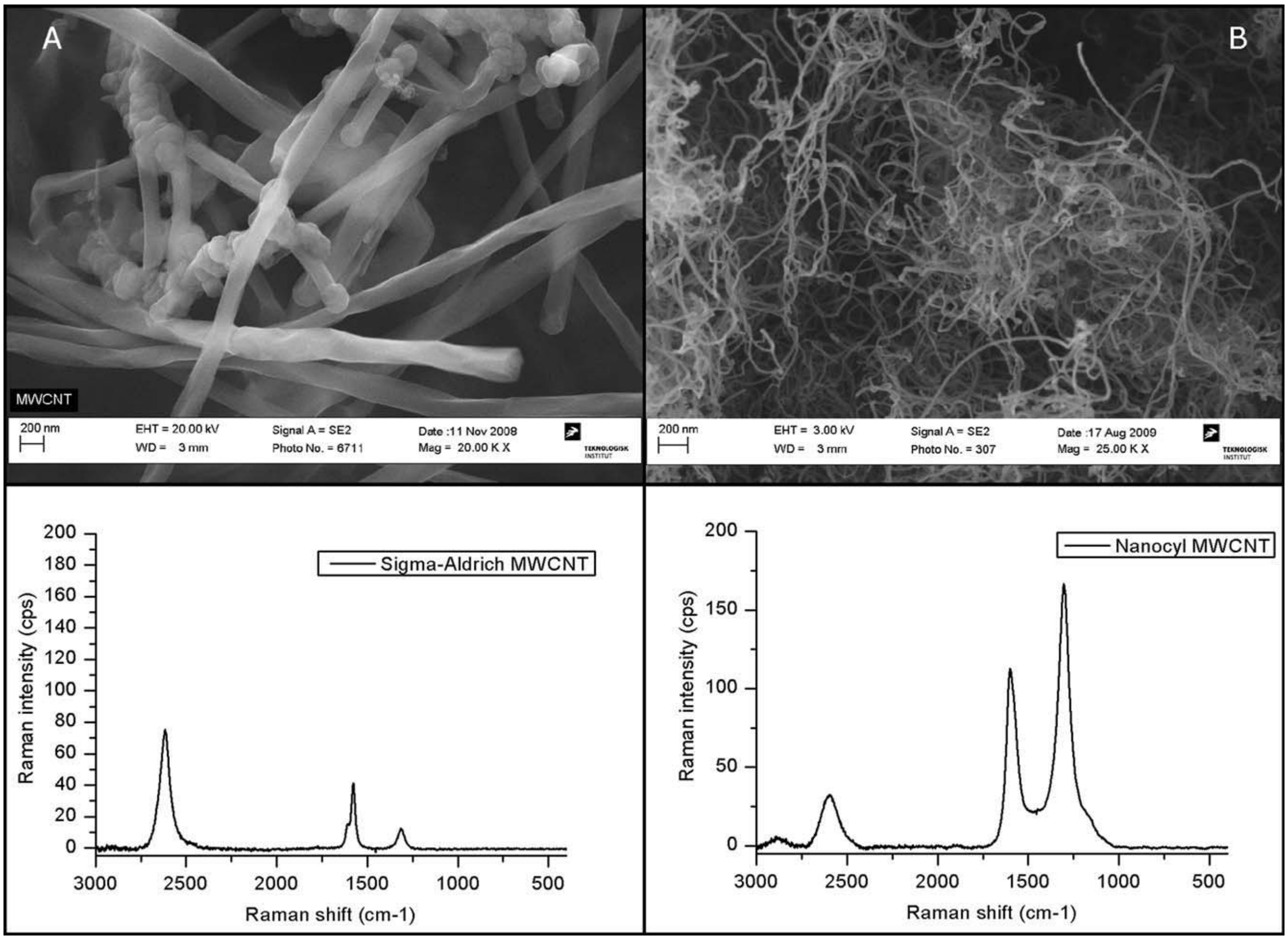

**FIGURE 1** Raman spectra and scanning electron micrographs of the two different grades of MWCNT. The left column shows data on the pristine MWCNT from Sigma-Aldrich (A), the right column shows data on the pristine MWCNT from Nanocyl (B).

at 1310 $cm^{-1}$. However, for the MWCNT from Sigma-Aldrich, the ratio of the D and G-band was found to be 0.43, whereas for the MWCNT from Nanocyl, it was found to be 1.94. This difference indicates that there are a large number of defects in the industrial grade MWCNT from Nanocyl, which would be expected of a lower quality material.

For modification of the MWCNT, it was decided to use a radical method, because these are independent of the former-mentioned acid treatments. A functional initiator based on a concept developed by Huang et al.[29] for surface grafting of polypropylene was adopted to functionalization of MWCNT as shown in Scheme 1.

Here, a UV sensitive ATRP initiator (**1**) was prepared directly from commercially available starting materials by an ester synthesis.[29] This initiator could then be covalently bound to the pristine MWCNT in dispersion by exposure to UV light (365 nm). Here, it is believed that a ketyl radical is formed through abstraction of a proton from either solvent (toluene)

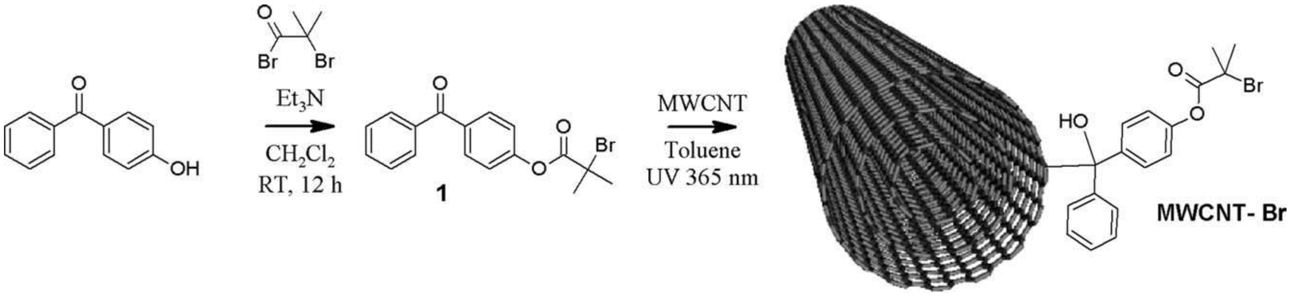

**SCHEME 1** Preparation of the UV sensitive ATRP initiator and subsequent reaction with MWCNTs under UV irradiation at 365 nm.

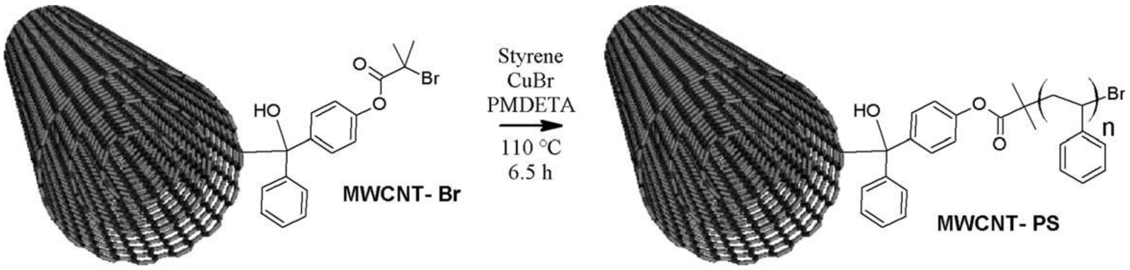

**SCHEME 2** ATRP of styrene from the initiator functionalized MWCNT-Br. TGA of such a sample is shown in Figure 2, where A is Sigma-Aldrich and B is Nanocyl.

or the defects on the nanotubes. Recombination or reaction with the nanotube affords the initiator functionalized material. Raman spectroscopy corroborates the introduction of the initiator onto the MWCNT. In the Raman spectra of the MWCNT-Br, there is an increase in the D-band relative to the G-band, indicating an increase in $sp^3$ hybridized carbon. On the Sigma-Aldrich MWCNT, this resulted in an increase in the peak intensity ratio $I_D/I_G$ from 0.43 to 0.49, whereas for Nanocyl's MWCNT the $I_D/I_G$ ratio was increased from 1.94 to 2.14. This indicates that the reactions are occurring on the sidewall and not only on defects, although it must be assumed that the reaction will occur at both defects and on the sidewall. If only defects were reacted no change would be observed in the Raman spectra from pristine to MWCNT-Br. Unfortunately, the loading of the initiator is too low to be detected from TGA analyses. Therefore, the prepared MWCNT-Br was used directly to initiate polymerizations of styrene in dispersion under standard ATRP conditions as shown in Scheme 2.

As can be seen, none of the pristine tubes show noteworthy weight loss in the analyzed region from room temperature to 700 °C, which indicates that the defects observed from Raman spectroscopy are not low-molecular weight carbon material. After the polymerizations have been performed, there is an increase in weight loss observed for both grades, although the increase is substantially higher for the industrial grade from Nanocyl. Pristine MWCNT exposed to the equivalent polymerization conditions afforded no increase in weight loss as determined by TGA for both grades of MWCNT. This clearly confirms that the increase in loading is due to polymer formed on or in proximity to the MWCNT, and thus corroborates the presence of the initiator on the tubes. If the initiator was only adsorbed and not covalently bound, the bulk of such free polymer would have been dissolved during the purification process. This would result in a much lower loading of polymer than what is observed on the MWCNT from Nanocyl and in no loading of polymer on the MWCNT from Sigma-Aldrich. Adsorption experiments with free PS on both grades of MWCNT showed that the tubes from Sigma-Aldrich do not adsorb any free polymer from solution, whereas the MWCNT from Nanocyl shows some adsorption. However, even after long exposure times with a large excess of free polymer, the maximally possible adsorption was found to be 5–8 wt % PS. With the loading observed from TGA in Figure 2, it is clear that this can only be a result of the presence of covalently bound initiator on the MWCNT.

The chemical composition of the formed polymer was investigated by TGA-GC-MS of a small sample of MWCNT grafted with polymer. The sample was degraded by TGA, and

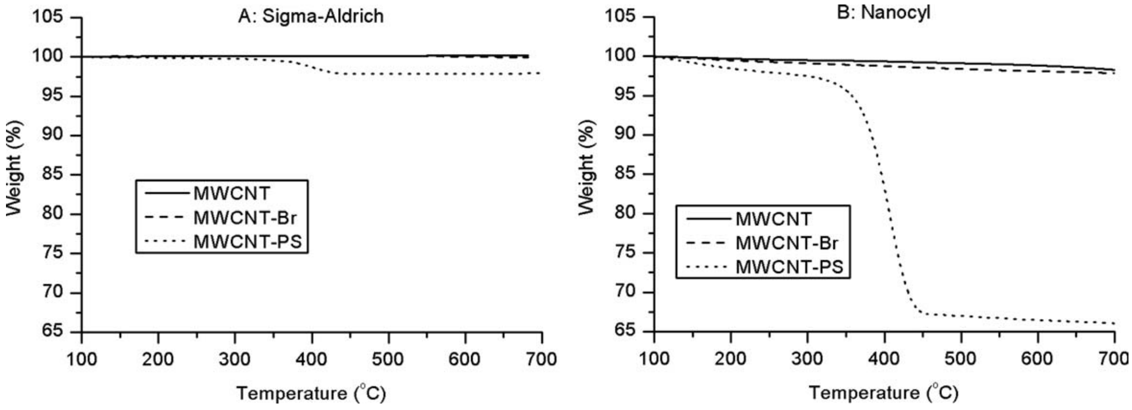

**FIGURE 2** TGA analyses of the two grades of MWCNT before and after introduction of the initiator and subsequent ATRP of styrene.

**TABLE 1** TGA Results Showing PS Loading Resulting From Variation in Polymerization Time and Ligands on the Two Different MWCNT-Br Batches

| | | TGA Mass Loss @ 460 °C After Different Polymerization Times (wt %) | | |
|---|---|---|---|---|
| MWCNT-Br | Ligand | 2.0 h | 6.5 h | 16.5 h |
| Sigma-Aldrich | dNbiPy | 0.7 | –[a] | 4.0 |
| Nanocyl | dNbiPy | 5.3 | 19.0 | 47.6 |
| Nanocyl | PMDETA | 20.2 | 54.0 | –[b] |
| Sigma-Aldrich | PMDETA | –[a] | 2.0 | –[a] |

[a] Samples were omitted as they were not necessary to compare with the equivalent Nanocyl sample.

[b] It was not possible to continue the polymerization due to high viscosity.

the corresponding off-gas was passed through adsorption columns for analysis by thermal desorption GC-MS. The collection of the degradation products was divided over temperature intervals corresponding to the weight loss steps detected in the TGA analysis. These investigations directly correlated the observed weight loss to PS from the grafting. The PS-grafted MWCNT (MWCNT-PS) were additionally attempted investigated by nuclear magnetic resonance spectroscopy (NMR), attenuated total reflection Fourier transform infrared spectroscopy (ATR-FT-IR), KBr pellets in transmission FT-IR and finally by Fourier transform photoacoustic infrared spectroscopy (FT-PAS-IR) to corroborate the structure. However, in our hands, these investigations were unsuccessful and yielded no useful analysis data. Especially, PAS-IR is a technique that has been known to give very good results on samples containing high amounts of carbon black and was expected to be well suited for analysis of functionalized CNT.[30] However, in this case even this method was unsuccessful.

The combined analysis results show that the method works and enables the preparation of MWCNT-PS through application of the UV initiator. After establishing the method, the polymerization time and the choice of ligands were optimized. Polymerizations were conducted with dNbiPy or pentamethyldiethylenetriamine (PMDETA) on both grades of tubes for different polymerization times. TGA of the prepared MWCNT-PS were used to determine the optimal reaction conditions as shown in Table 1.

Based on earlier experience where dNbiPy has shown superior properties in surface initiated ATRP,[31] it was decided to use this ligand for the first polymerizations. Even after repeated experiments and longer reaction times, it was found to be impossible to obtain more than a 4.0 wt % loading of polymer on the MWCNTs from Sigma-Aldrich (determined by TGA). Even though this was disappointing, the experiment was repeated for comparative reasons on the MWCNTs from Nanocyl. Surprisingly, the exact same method resulted in a loading of up to 47.6 wt % after 16.5 h under the same conditions. Therefore, it was decided to test these tubes with a different ligand, PMDETA, and otherwise unchanged reaction conditions. With PMDETA and Nanocyl's tubes, it was possible to obtain the highest loading of all cases after only 6.5 h of reaction with 54.0 wt % polymer. The comparative experiment on the tubes from Sigma-Aldrich resulted only in a 2.0 wt % loading of polymer. It is quite clear that the industrial grade tubes from Nanocyl give a much higher loading compared to the tubes from Sigma-Aldrich under all conditions. This could be an effect of both the much higher aspect ratio in these tubes (160 versus 50), resulting in a larger surface area or an effect of the amount of defects as illustrated by Raman spectroscopy in Figure 1. This large difference in loading illustrates the importance of characterization of the starting material before functionalization to be able to evaluate the efficiency of different methods of grafting, a property that is often neglected. In addition to the effect of different tubes, the choice of ligand has also been found to have a substantial influence on the polymer

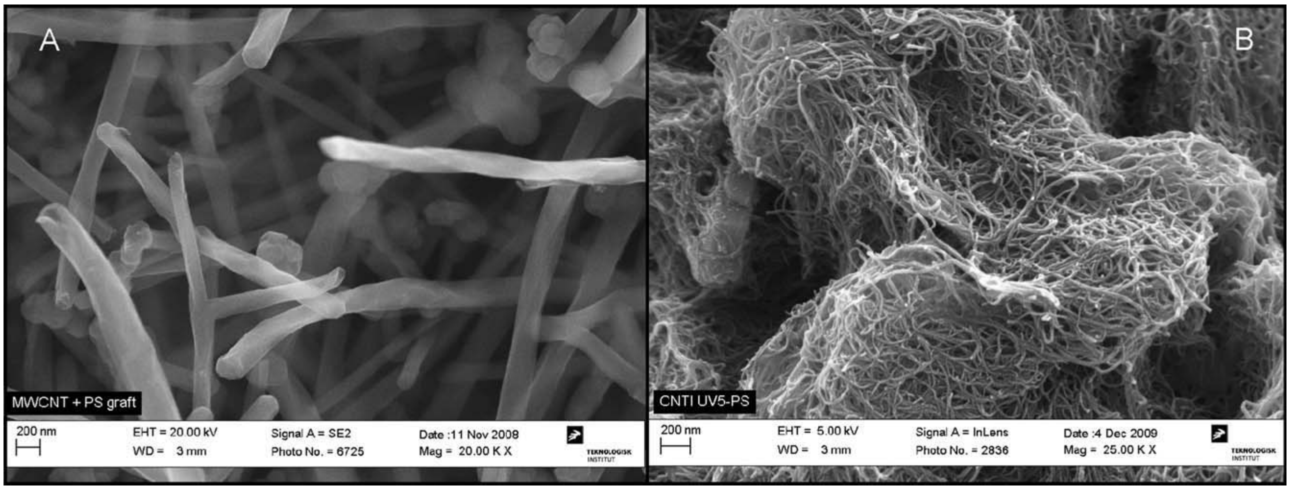

**FIGURE 3** Scanning electron micrographs of polystyrene-grafted MWCNT, A: Sigma-Aldrich MWCNT-PS, B: Nanocyl MWCNT-PS.

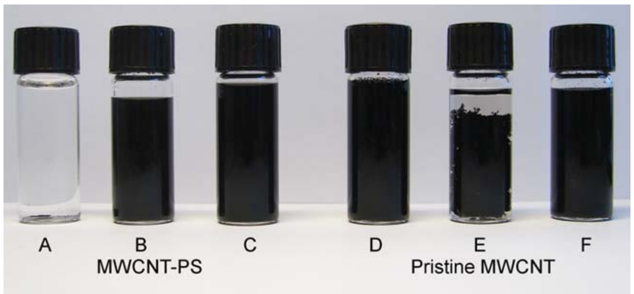

**FIGURE 4** Dispersion experiments of MWCNT-PS (Nanocyl, A-C) compared with pristine MWCNT (Nanocyl, D-F) 1.5 h after dispersion. The dispersions have been prepared at 20 °C in cyclohexane (A,D), dichloromethane (B,E), and dioxane (C,F) with a concentration of 0.5 mg/mL.

loading. This is not surprising because it is well known from ATRP that the ligand has a large influence on polymerizations. However, it is interesting that dNbiPy that has been found to show superior performance on other surfaces in this case performs worse than PMDETA.

Samples of the PS-grafted MWCNTs were investigated by SEM, resulting in the micrograph shown in Figure 3.

Because of the low loading on the Sigma-Aldrich tubes, the micrograph shows no substantial difference compared with the unfunctionalized one in Figure 1. In the case of the Nanocyl tubes, it is clear that a substantial loading has been obtained resulting in a matrix of polystyrene enveloping the tubes. This was corroborated through a dispersion experiment in cyclohexane, dichloromethane, and dioxane as shown in Figure 4.

As can clearly be seen, the grafting of the tubes have had a substantial influence on solubility. The functionalized material is completely indispersable in cyclohexane at 20 °C and dispersible in dichloromethane in contrary to the pristine material, whereas the dispersability in dioxane was unchanged. Similar results were observed for dispersion experiments on the PS-grafted MWCNT from Sigma-Aldrich.

DSC investigations of the prepared MWCNT-PS showed glass transition temperatures in the range of 107–110 °C. These high glass transition temperatures indicate that the PS is attached to the surface of the MWCNT where the proximity to the rigid MWCNT restricts rotation and thereby results in a higher glass transition temperature compared with free PS prepared by ATRP.[32] This has also been observed by Viswanathan et al.,[33] who showed that only covalently bound PS gave rise to such an increase in glass transition temperature on SWCNT.

To estimate the molecular weight of the grafted chains, a hydrolysis experiment was performed on the MWCNT-PS. Because of the low loading observed on Sigma-Aldrich tubes, it was not possible to do this on these samples. However, it was done on the MWCNT-PS prepared from Nanocyl's tubes. Here SEC analysis showed that the hydrolyzed polymer had a $M_n$ = 39,600 g/mol (PDI = 1.5) for a sample with 47 wt % polymer.

The general method is also applicable for other monomers, which was illustrated by a polymerization of the hydrophilic monomer PEGMA. This resulted in a grafting of 4.6 wt % of poly(PEGMA) onto the MWCNT from Sigma-Aldrich, which corresponds to loading obtained with styrene. The poly(PEGMA) grafting had an obvious influence on the solubility, where the functionalized MWCNT could be dispersed in MeOH, which is in clear contrast to the pristine and initiator functionalized MWCNT that were indispersable in MeOH.

Finally, the prepared MWCNT-PS was applied in new composite materials based on polyphenylenesulfide (PPS). Because PS and PPS are miscible, it was intended to exploit the PS functionalization of the MWCNT to compatibilize the nanotubes to the matrix. Because PPS is insoluble such a composite needs to be prepared by extrusion, and it was decided to test the dispersion of the MWCNT-PS in a soluble polymer (PS) first to simplify the system.

Model composites were solution casted from toluene and dioxane and investigated by rheology at elevated temperatures. The degree of CNT dispersion in PS was found by evaluation of the low-frequency behavior of the storage modulus,

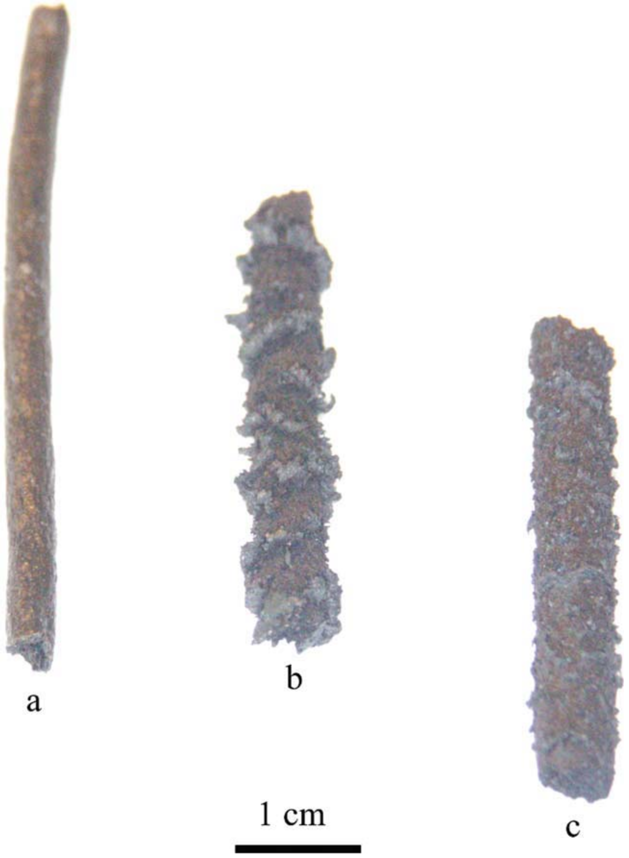

**FIGURE 5** Extruded samples of a standard PPS (a), a PPS composite with pristine MWCNT (b) and a PPS composite with MWCNT-PS (c).

G′, measured from small amplitude oscillatory shear. Samples with well-dispersed nanotubes are known to display a non-terminal G′ at low frequencies, as compared with samples with poorly dispersed nanotubes and pure polymer melts. This effect is caused by a formation of nanotube networks that restrains the motions of the polymer chains.[34] The oscillatory shear rheology measurements confirmed a good dispersion of the MWNCT-PS in the PS matrix, and the nanotubes were consequently applied for preparation of the PPS-(MWCNT-PS) composite prepared by mixing during extrusion. Three different samples were extruded as shown in Figure 5 where an ordinary PPS, a masterbatch with 2.5 wt % of pristine MWCNT and a masterbatch with 2.5 wt % of PS-grafted MWCNTs are compared.

It is clear that the functionalized MWCNT has a large influence on the structure of the extruded samples. In the masterbatch of the pristine MWCNT, the structure of the PPS was very rough and the sample seemed very brittle, whereas the composite made from the modified MWCNT was much smoother and less brittle although still rougher than the ordinary PPS. The masterbatches have been used for preparation of composites with a varied content of MWCNT and the mechanical properties are currently under investigation.

## CONCLUSIONS

PS-functionalized MWCNT were prepared through a novel UV-initiated radical method for CNT materials. Polymerization of styrene by ATRP was optimized with two different ligands, and PMDETA was found to show superior properties, resulting in the largest loading and the shortest polymerization time. The procedure was used to prepare PS-grafted MWCNT based on two different batches of tubes. This illustrated large differences in the MWCNT starting materials underlining the importance of proper characterization of the starting materials. In addition to this, the method was also applied for PEGMA, resulting in grafted MWCNT that were much easier to disperse in polar solvents. The prepared PS-grafted MWCNTs were finally applied in composites of PS or PPS, and these samples showed clear indications of the effect of modification on the quality of the composites.

The authors acknowledge the Innovation Consortium "Extreme Materials for Extreme Environments" funded by the Danish Ministry of Science Technology and Innovation under contract 08-034101 for financial support. Louise Kjærulff and Ulrich Berner are acknowledged for synthesis work as part of internships at the Danish Polymer Centre, Department of Chemical and Biochemical Engineering at the Technical University of Denmark (DTU). Laboratory technician Kim Chi Szabo performed the thermal analyses at DTU. Kathrine Bjørnboe acquired SEM and Eva Pedersen performed the GC-MS analyses at the Danish Technological Institute.

## REFERENCES AND NOTES

**1** Moniruzzaman, M.; Winey, K. I. Macromolecules 2006, 39, 5194–5205.

**2** Grady, B. P. Macromol Rapid Commun 2010, 31, 247–257.

**3** Yan, Y. H.; Zhao, S. A.; Cui, J.; Yang, S. B. J Polym Sci Part A: Polym Chem 2009, 47, 6135–6144.

**4** Lafuente, E.; Pinol, M.; Martinez, M. T.; Munoz, E.; Oriol, L.; Serrano, J. L. J Polym Sci Part A: Polym Chem 2009, 47, 2361–2372.

**5** Jeon, I. Y.; Tan, L. S.; Baek, J. B. J Polym Sci Part A: Polym Chem 2008, 46, 3471–3481.

**6** Singh, P.; Campidelli, S.; Giordani, S.; Bonifazi, D.; Bianco, A.; Prato, M. Chem Soc Rev 2009, 38, 2214–2230.

**7** Tasis, D.; Tagmatarchis, N.; Bianco, A.; Prato, M. Chem Rev 2006, 106, 1105–1136.

**8** Homenick, C. M.; Lawson, G.; Adronov, A. Polym Rev 2007, 47, 265–290.

**9** Qin, S. H.; Qin, D. Q.; Ford, W. T.; Resasco, D. E.; Herrera, J. E. Macromolecules 2004, 37, 752–757.

**10** Pei, X. W.; Xia, Y. Q.; Liu, W. M.; Yu, B.; Hao, J. C. J Polym Sci Part A: Polym Chem 2008, 46, 7225–7237.

**11** Liu, Y. L.; Chen, W. H. Macromolecules 2007, 40, 8881–8886.

**12** Wu, H. X.; Tong, R.; Qiu, X. Q.; Yang, H. F.; Lin, Y. H.; Cai, R. F.; Qian, S. X. Carbon 2007, 45, 152–159.

**13** Baskaran, D.; Mays, J. W.; Bratcher, M. S. Angew Chem Int Ed Engl 2004, 43, 2138–2142.

**14** Kong, H.; Gao, C.; Yan, D. Y. J Am Chem Soc 2004, 126, 412–413.

**15** Hou, J. Q.; Zhou, X. D.; Sui, Z. J.; Zhou, X. G. Polym Int 2009, 58, 564–569.

**16** De Falco, A.; Fascio, M. L.; Lamanna, M. E.; Corcuera, M. A.; Mondragon, I.; Rubiolo, G. H.; D'Accorso, N. B.; Goyanes, S. Physica B 2009, 404, 2780–2783.

**17** Ryu, J.; Ramaraj, B.; Yoon, K. R. Surf Interface Anal 2009, 41, 303–309.

**18** Llarena, I.; Romero, G.; Ziolo, R. F.; Moya, S. E. Nanotechnology 2010, 21, 055605 (8 pp).

**19** Zhu, L. Z.; Jin, Q.; Xu, J. P.; Ji, J.; Shen, J. C. J Appl Polym Sci 2009, 113, 351–357.

**20** Zhao, X. D.; Fan, X. H.; Chen, X. F.; Chai, C. P.; Zhou, Q. F. J Polym Sci Part A: Polym Chem 2006, 44, 4656–4667.

**21** Cui, J.; Wang, W. P.; You, Y. Z.; Liu, C. H.; Wang, P. H. Polymer 2004, 45, 8717–8721.

**22** Hong, C. Y.; You, Y. Z.; Pan, C. Y. Polymer 2006, 47, 4300–4309.

**23** Priftis, D.; Sakellariou, G.; Baskaran, D.; Mays, J. W.; Hadjichristidis, N. Soft Matter 2009, 5, 4272–4278.

**24** Priftis, D.; Sakellariou, G.; Hadjichristidis, N.; Penott, E. K.; Lorenzo, A. T.; Muller, A. J. J Polym Sci Part A: Polym Chem 2009, 47, 4379–4390.

**25** Liu, Y. L.; Chen, W. H.; Chang, Y. H. Carbohydr Polym 2009, 76, 232–238.

**26** Liu, J. Y.; Nie, Z. H.; Gao, Y.; Adronov, A.; Li, H. M. J Polym Sci Part A: Polym Chem 2008, 46, 7187–7199.

**27** Sui, K. Y.; Yang, C. J.; Gao, S.; Shan, X.; Xia, Y. Z.; Zheng, Q. J Appl Polym Sci 2009, 114, 1914–1920.

**28** Fragneaud, B.; Masenelli-Varlot, K.; Gonzalez-Montiel, A.; Terrones, M.; Cavaille, J. Y. Chem Phys Lett 2006, 419, 567–573.

**29** Huang, J. Y.; Murata, H.; Koepsel, R. R.; Russell, A. J.; Matyjaszewski, K. Biomacromolecules 2007, 8, 1396–1399.

**30** Grose, R. I.; Hvilsted, S.; Siesler, H. W. Makromol Chem Macromol Sympos 1991, 52, 175–189.

**31** Jankova, K.; Nguyen, K. C.; Chen, X. Y.; Kops, J.; Johannsen, I.; Batsberg, W. Abstracts of Papers of the American Chem Society 1998, 216, 109-POLY.

**32** Plackett, D.; Jankova, K.; Egsgaard, H.; Hvilsted, S. Biomacromolecules 2005, 6, 2474–2484.

**33** Viswanathan, G.; Chakrapani, N.; Yang, H. C.; Wei, B. Q.; Chung, H. S.; Cho, K. W.; Ryu, C. Y.; Ajayan, P. M. J Am Chem Soc 2003, 125, 9258–9259.

**34** Zhang, Q. H.; Fang, F.; Zhao, X.; Li, Y. Z.; Zhu, M. F.; Chen, D. J. J Phys Chem B 2008, 112, 12606–12611.